

The Effects of Prolonged Temporal Modulation on the Differential Response of Color Mechanisms

ARTHUR G. SHAPIRO,* QASIM ZAIDI*

Received 30 March 1992; in revised form 15 May 1992

The identification of three independent cardinal directions in color space suggests the existence of three independent post-receptoral mechanisms that can be desensitized by habituation to a temporally modulated light. In this paper, the differential response of each cardinal mechanism is estimated over a range of inputs before and after habituation. Simple mathematical considerations show that the threshold elevations following temporal modulation are not consistent with multiplicative gain changes; rather, these elevations require a change in the shape of each cardinal mechanism's response function. With this method, the effects of habituation can also be differentiated from the effects of a change in the steady adapting light.

Color vision Habituation Adaptation Sensitivity Gain control

INTRODUCTION

Prolonged viewing of a light whose color is modulated in time changes an observer's sensitivity to color differences—an effect which we will refer to as habituation. In this paper, we derived the functional properties of the processes mediating this effect by comparing empirical estimates of differential sensitivity to predictions of explicit mathematical models. In addition, we compared the changes that occur following habituation to those that occur following a shift in the color of the steady adapting light.

Krauskopf, Williams and Healy (1982) used habituation to prolonged temporal modulation to delineate three independent cardinal axes in color space. They measured thresholds for discriminating probes from a mid-white background before and after exposure to a light whose color was modulated sinusoidally in time. They found that after exposure to a light whose color was modulated along a cardinal axis, thresholds were elevated when the probes differed from white along the axis of modulation, but remained unchanged for probes that differed from white along the other two cardinal axes. When the habituating light was modulated along any other line in the three planes formed by the cardinal axes, thresholds were elevated in all directions within that plane. This selective elevation indicates that, with respect to color habituation, there are three orthogonal directions in color space.

In this paper, the three cardinal axes will be called *YV*, *RG*, and *LD* and are shown as the axes of the three-dimensional color space in Fig. 1. The center of this space is an achromatic light, *W*. Lights represented by different points along the *YV* axis are indistinguishable for the L- and M-cones and differ only in S-cone excitation; changes along this axis from *Y* to *V* increase the S-cone excitation linearly. Lights represented by points on the *RG* axis are indistinguishable for the S-cones and differ only in L- and M-cone excitation; changes along this axis trade off the L- and M-cone excitations in such a way that their sum remains constant. The *LD* axis depicts a set of achromatic lights such that the excitation of all three cones increases proportionately from *D* to *L*.

The habituation results of Krauskopf *et al.* (1982) are consistent with the existence of three independent classes of cardinal mechanisms, such that modulation along a cardinal axis stimulates only one class. Consequently, each class of mechanism can be defined by the absence of a response to modulation along two of the cardinal axes and, to any modulation in the color plane formed by them. Any plane in color space can be defined by an equation of the form

$$aL \pm bM \pm cS = 0, \quad (1)$$

where *L*, *M*, and *S* are the spectral sensitivities of the cones, and *a*, *b*, and *c* are three positive real constants. Consequently, if each cardinal mechanism has a plane in color space to which its response is zero, then its response can be expressed either as a linear combination of cone absorptions or as a linear or nonlinear operation

*Department of Psychology, Columbia University, New York, NY 10027, U.S.A.

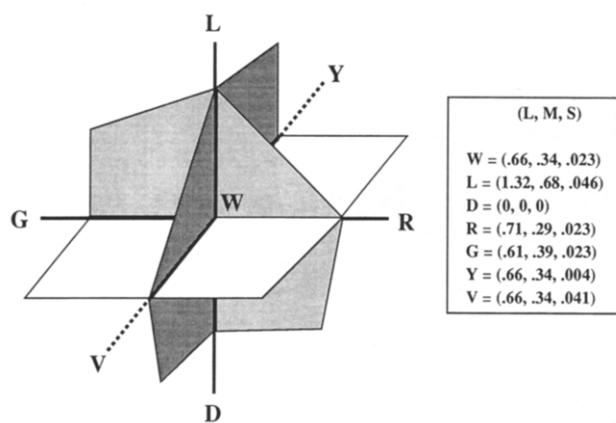


FIGURE 1. Color space specified in terms of the cardinal axes. The LD - YV plane is shaded dark; the LD - RG plane, gray; and the RG - YV plane, white. W represents mid-white at 50 cd/m^2 . The numbers represent L -, M -, and S -cone excitations at the end of each axis. These numbers correspond to "r," "g," and "b" of MacLeod and Boynton (1978) and are the maximal range permitted by the equipment. Reproduced with permission from Sachtler and Zaidi (1992).

on this combination. In terms of cone units in Fig. 1, the linear combinations, C , defining the response of the three cardinal mechanisms are as follows:

- (i) For the mechanism that responds to changes along the LD axis but not along the RG - YV plane,

$$C = L + M. \quad (2a)$$

- (ii) For the mechanism that responds to changes along the YV axis but not along the RG - LD plane,

$$C = S - 0.023(L + M). \quad (2b)$$

- (iii) For the mechanism that responds to changes along the RG axis but not along the YV - LD plane,

$$C = L - 1.94M. \quad (2c)$$

The habituation experiment of Krauskopf *et al.* (1982) identified color mechanisms that changed their sensitivity in response to repeated temporal transitions of the input. Changes in color thresholds also occur with changes in the color of the steady adapting light. In previous work (Zaidi, Shapiro & Hood, 1992; Shapiro, Zaidi & Hood, 1990), we developed a method to study these shifts in sensitivity. In each state of adaptation, we measured the differential sensitivity of a cardinal mechanism over an extended range. Sensitivity at the adaptation state was measured by means of difference-thresholds on the steady background. Sensitivity over a larger range was measured by means of difference-thresholds on briefly flashed backgrounds that were different from the adapting light. Because the probe and flashed backgrounds were presented for an interval too short to disturb the state of adaptation, any changes in threshold could be attributed to static response limitations rather than adaptive processes. We estimated a static input-response function for the cardinal mechanism from the differential-sensitivity curves measured in each adaptation state. By examining how the response functions changed as a function of adaptation state, we

were able to infer the nature of the underlying adaptation processes. The experimental and conceptual bases of these experiments were extensions of previous work by Wright (1935), Craik (1938), Hood, Finkelstein and Buckingham (1979), Geisler (1979), Loomis and Berger (1979), and Adelson (1982).

In the present study, we were mainly interested in the effect of habituation on the response properties of the cardinal mechanisms. In particular, we were interested in whether the effect of habituation could be characterized by a multiplicative scaling of the chromatic signal at some stage in the visual process. In order to investigate this, we measured the extended differential sensitivity curve during adaptation to a steady white light and following exposure to a temporally modulated light. In a variation of the method we had used to study the effect of changes in the steady adaptation color, we derived static input-response functions in both pre- and post-habituation conditions. Predictions about the change in the differential sensitivity curves from simple mathematical models showed that the effect of habituation could not be characterized by a multiplicative scaling of the chromatic signal at any stage in the visual process but instead required a change in the shape of the cardinal mechanism's response function.

In addition, we show that the effects of prolonged temporal modulation on sensitivity to color differences are qualitatively different from the effects of changes in the color of a steady adapting light. In previous work we showed that when an observer is adapted to mid-white, difference-threshold curves measured along a cardinal axis have a "V" shape with a minimum at the adapting background. When the observer adapts to a steady light on the same cardinal axis, the change in the difference-threshold curves can be described mainly by a lateral shift so that the minimum is at or near the adaptation point (Shapiro *et al.*, 1990; Zaidi *et al.*, 1992). Following habituation, however, the minimum in the difference-threshold curve remains at white, but the curve is elevated and flatter relative to the pre-habituation curve. Therefore, the change in sensitivity following habituation must be due to different processes than those that tune differential sensitivity for a steady adapting light.

METHODS

Specification of colors

The range of stimuli used in this experiment is depicted in Fig. 1. Colors are specified in terms of the cardinal axes, labeled YV , RG , and LD . The three axes are centered at W , an achromatic light of 50 cd/m^2 . The numbers in the table to the right of the figure show the values of the Smith and Pokorny (1975) cone excitations at the ends of each axis. These excitations correspond to the "r," "g," and "b" units of the MacLeod and Boynton (1979) chromaticity diagram. The edges of the plane show the maximum range permitted by the equipment used in this study. The letters at the end of the axes are for mnemonic convenience only.

Equipment

Stimuli were displayed on the screen of a Tektronix 690SR color television monitor. The screen was refreshed at 120 interlaced frames per sec. Images were generated using an Adage 3000 raster-based frame buffer generator. The Adage allowed for ten-bit specification of the output of each TV gun, leading to a palette of 2^{30} possible colors, of which 256 could be displayed on any one frame. The computer controlled all stimulus generation and data collection. Detailed calibration procedures are discussed in Zaidi *et al.* (1992) and Zaidi and Halevy (1992).

Observers

The data presented here are for one of the authors (AGS), who has normal acuity and color vision as assessed by Farnsworth–Munsell 100-hue and Rayleigh tests, and a second observer (KB), a female, had no prior psychophysical experience and did not know the aims of this study.

Procedure

Each session consisted of two types of trials: pre-habituation trials, in which difference-thresholds were measured during exposure to a steady white background; and post-habituation trials, in which difference-thresholds were re-measured following exposure to a temporally modulated field.

The temporal sequence and spatial configuration of the stimuli in the pre-habituation trials are shown in Fig. 2(a). In these trials, the observer fixated on a spot in the center of a steady square field (10 deg on each side), metameric to W at 50 cd/m², for an adaptation period of 120 sec. The color of the square field was kept at the adaptation color (W) for an additional period of

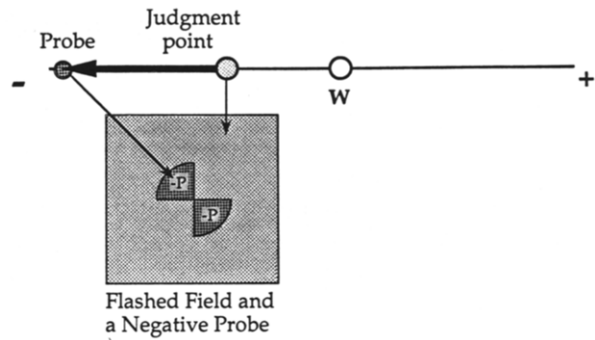


FIGURE 3. Judgment point and probe represented as points on the cardinal axis. On this axis, the open circle indicates the adaptation point, the lightly shaded circle indicates the location of a judgment point, and the darker circle indicates the location of the probe. In the figure, the judgment point is on the negative side of W , and the probe is a negative excursion from the judgment point along the cardinal axis. A staircase procedure measured the distance at which the probe could be discriminated from the fixed judgment point 71% of the time.

0.6 sec, and then changed to the color of the flashed background for 0.5 sec. For the first 0.05 sec of the flashed interval, a probe was presented as two quadrants of a disk, 3 deg in diameter, centered at the fixation spot. Subsequent presentations of the probe and flash were preceded by a 10 sec presentation of the adapting stimulus. The observer could discriminate the probe from the flash only during the 0.05 sec interval. We chose this length as being short enough not to disturb the adaptation state, but long enough to measure chromatic thresholds in a wide range of conditions. The butterfly shape of the probe was chosen over the usual circular shape for two reasons: (i) with a circular probe, discrimination from the flash takes place on the outer edge of the probe, but with the butterfly shape the center of the fovea can be used for discrimination; and (ii) a roughly circular Maxwell's spot—transiently visible for some of the flashes used in this experiment—would have interfered with judgments about the presence or absence of a circular probe.

The spatial configuration and temporal sequence for the post-habituation trials are shown in Fig. 2(b). During the habituation phase, the color of the square field was modulated sinusoidally at 1 Hz along one of the cardinal axes. The modulation was symmetric around W , and its amplitude was the maximum range permitted by the monitor's phosphors. Initial exposure to the habituating stimulus lasted for 120 sec. This was followed by a 0.6 sec presentation of a steady white field and then by the combination of the probe and the flashed field. The probe and the flashed field had the identical spatial configuration and temporal duration used in the pre-habituation tests. Subsequent presentations of the delay, probe, and the flash were preceded by 10 sec of top-up habituation.

In each experiment, the flashed fields were lights metameric to points on a cardinal axis. These points are referred to as judgment points. A probe was an excursion from the judgment point in one direction along the same cardinal axis. Figure 3 depicts the conditions for one trial. Along a cardinal axis, the open circle shows the

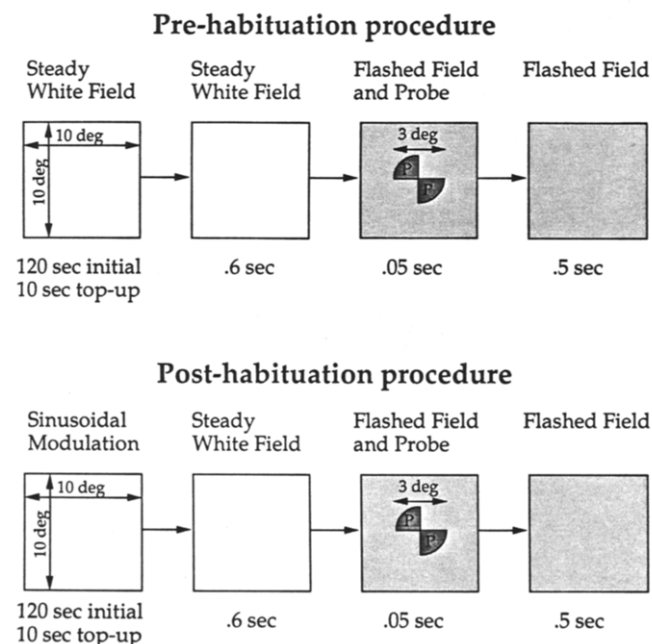


FIGURE 2. Spatial configuration and temporal sequence of stimuli for (a) the pre-habituation procedure and (b) the post-habituation procedure. See text for description.

adapting color, W . The flashed judgment point is shown as a lightly shaded circle, and the probe as a darker circle.

Observer AGS responded "yes" if the observer could discriminate the probe from the flashed background, or "no" if the probe and flash were indistinguishable. For each flash condition, two randomly interleaved staircases tracked the 71% point on the psychometric curve by decreasing the distance between the probe and the judgment point if the observer could distinguish the probe from the flashed background on two consecutive presentations within a staircase, and increasing the distance if the observer could not distinguish the probe from the flashed background on any presentation. This distance was referred to as a difference-threshold. A transition was said to occur when the distance was increased following a sequence of decreases, or decreased following a sequence of increases. The value of each difference-threshold was the mean of twelve such transitions (Wetherill & Levitt, 1965). Each trial consisted of randomly interleaved measurements for either two or four judgment points symmetric around W . The data for observer KB was collected using a two-alternative forced choice (2AFC) condition and bidirectional probes.

Equiluminance along the color lines was checked for each observer with flicker photometry. It is unlikely that luminance artifacts affect the chromatic probe thresholds since for this spatial-temporal configuration chromatic flashes did not alter light-dark thresholds (Zaidi & Hood, 1988).

EXPERIMENT 1: HABITUATION ALONG THE YV AXIS

In the first experiment, the judgment points were spaced along the YV axis. Thresholds were measured for probes that differed from these points in either the positive or negative direction on the YV axis. The pre-habituation thresholds were measured during adaptation to a steady white background, and the post-habituation thresholds following habituation to a light modulated sinusoidally along the length of the YV axis. Figure 4 shows the difference-thresholds measured at each of the judgment points. The judgment points are represented in terms of their distance from W ; difference-thresholds, in terms of the distance between the probe and the judgment point. Since the L- and M-cone excitations stay the same along the entire YV axis, the judgment points and difference-thresholds can be described by the change in S-cone excitation (ΔS) alone. Figure 4(a) shows the thresholds for $+\Delta S$ probes, while Fig. 4(b) shows the thresholds for $-\Delta S$ probes. The solid circles indicate the pre-habituation thresholds, and the open circles, the post-habituation thresholds. The standard error of each point is between 10 and 20% of the threshold value.

For both positive and negative probes, the pre-habituation difference-thresholds are minimum at W and increase approximately linearly with the distance of the judgment point from W . The slopes of these curves are

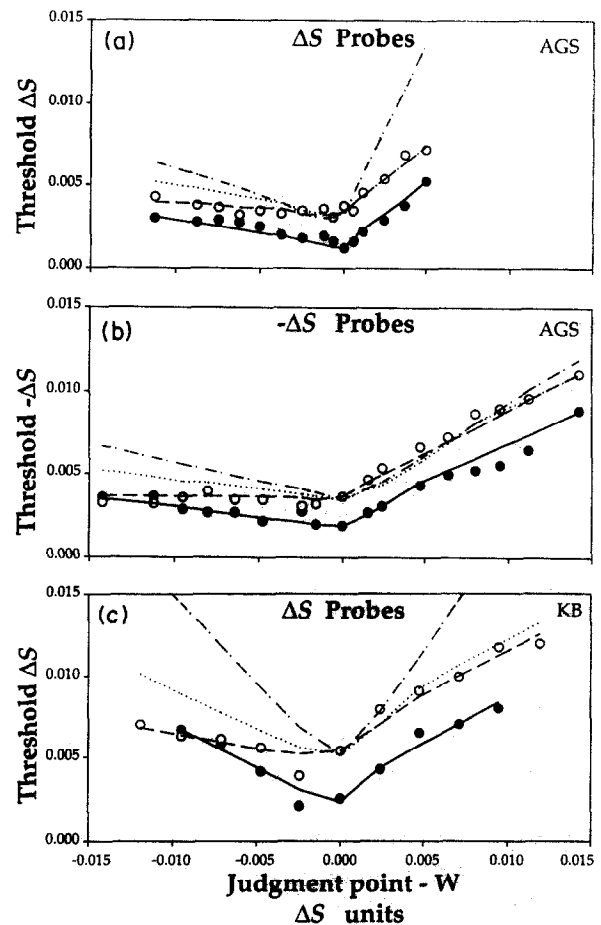


FIGURE 4. Difference-thresholds as a function of the judgment point's distance from W along the YV axis in ΔS units. (a) Difference-thresholds for probes differing from the judgment point in the positive direction of the YV axis. The solid circles indicate pre-habituation difference-thresholds; the open circles indicate post-habituation difference-thresholds. The solid line represents the predictions of the pre-habituation model; the dotted line, of post-habituation Model 1; the dot-dashed line, of post-habituation Model 2; and the dashed line, of post-habituation Model 3. (b) The difference-thresholds that differ from the judgment point in the negative direction of the YV axis. The lines represent predictions from the same models with the parameters estimated for this condition. (c) A replication of the results on a second observer using bi-directional probes and a 2AFC task.

steeper on the positive side of W than on the negative side. The post-habituation difference thresholds are elevated at W relative to the pre-habituation thresholds. On the positive side of W , the post-habituation curve increases with approximately the same slope as the pre-habituation curve; on the negative side of W , the slope is flatter than the pre-habituation curve. The data for the second observer [Fig. 4(c)] show similar effects.

MODELS OF DIFFERENTIAL SENSITIVITY AND HABITUATION

In this section we present a series of simple models to provide a mechanistic account for the experimental results. First, we described a model for the pre-habituation condition and then three alternate models for the effects of habituation. All of these models assume that under the present experimental conditions, sensitivity is limited at a single stage of the visual system

following the combination of cone signals. For thresholds along the *YV* and *RG* axes, a justification of this assumption is provided by Zaidi and Hood (1988) and Zaidi *et al.* (1992).

Model for differential-sensitivity in the pre-habituating condition

Because the pre-habituating thresholds were all measured in the same state of steady adaptation, we assume that thresholds are higher for judgment points further from the adaptation point because of a static response limitation in the cardinal mechanism. Figure 5(a) shows a schematic of a simple model that illustrates this assumption. In this model, the input to the cardinal mechanism is a linear combination of cone signals. For the *YV* mechanism, this combination is equal to $S - (L + M)$. The static response limitation is assumed to occur after the combination and is represented by a non-linear function. In order to predict approximately linear threshold curves, this non-linear relationship between input and response is assumed to be logarithmic:

$$R(C) = \frac{1}{\beta} \ln[\alpha + \beta(C - C_w)] - \frac{1}{\beta} \ln(\alpha) \quad (3)$$

R is the response of this stage, C is the combination of cone signals for the test color, C_w is the combination of cone signals at W , and α and β are the two free

parameters that completely determine the response function. For each mechanism, the values of C and C_w are determined from equations (2a, b and c). When the test color is W the value of the response in equation (3) is equal to zero.

Difference-thresholds are predicted from the response of the model by the assumption that a probe can be discriminated from the background only if the response to the superimposed probe and flash, minus the response to the flashed background alone, is equal to at least one unit; i.e. at threshold,

$$|R(F + P) - R(F)| = 1. \quad (4)$$

In the model, the value of the flashed background, F , was expressed in terms of the change of the flashed background from the mid-white adapting background, and the value of the probe, P , in terms of the difference between the probe and the flashed background.

Using equations (3) and (4), we derived an expression for the threshold value of the probe (P^*). If $F \geq 0$ and $P > 0$, then $R(F) > 0$ and $R(F + P) > R(F)$. Therefore, at threshold

$$\frac{1}{\beta} \ln[\alpha + \beta(F + P^*)] - \frac{1}{\beta} \ln(\alpha) - \left[\frac{1}{\beta} \ln(\alpha + \beta F) - \frac{1}{\beta} \ln(\alpha) \right] = 1. \quad (5)$$

By simple algebraic manipulations,

$$P^* = \frac{\alpha}{\beta} (e^\beta - 1) + (e^\beta - 1)F. \quad (6)$$

There are three other variants of this derivation for different combinations of positive and negative values of F and P :

for $F < 0$ and $P > 0$,

$$P^* = \frac{\alpha}{\beta} (e^{-\beta} - 1) + (e^{-\beta} - 1)F \quad (7)$$

for $F \geq 0$ and $P < 0$,

$$P^* = -\frac{\alpha}{\beta} (e^{-\beta} - 1) - (e^{-\beta} - 1)F \quad (8)$$

for $F < 0$ and $P < 0$,

$$P^* = -\frac{\alpha}{\beta} (e^\beta - 1) - (e^\beta - 1)F. \quad (9)$$

Equations (6)–(9) predict that P^* is a linear function of F . Estimates of α and β can be obtained by equating the expressions for the slope and the intercept in the equations to the slope and the intercept of the empirical threshold curve. For instance, in the condition where $F > 0$ and $P > 0$, we used equation (6) to get the following expressions for the estimates, $\hat{\alpha}$ and $\hat{\beta}$:

$$\hat{\alpha} = \hat{\beta} \frac{\text{Intercept}_{\text{pre}}}{e^{\hat{\beta}} - 1}. \quad (10a)$$

and

$$\hat{\beta} = \ln(\text{Slope}_{\text{pre}} + 1); \quad (10b)$$

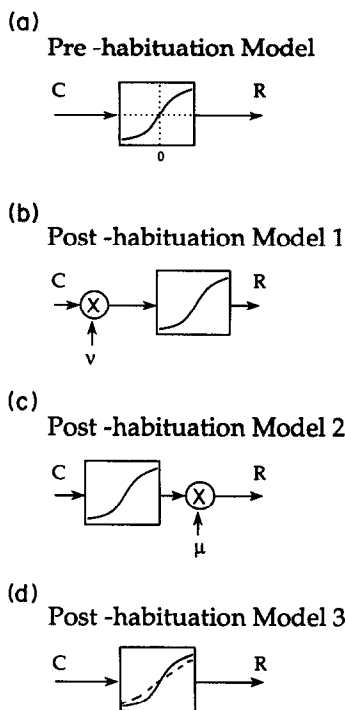


FIGURE 5. Schematic of pre- and post-habituating models. (a) The pre-habituating model. The response of the cardinal mechanism is a logarithmic function of the input. The parameters of the function are estimated from the pre-habituating data. (b) Post-habituating Model 1. The input signal is multiplied by a scalar, $v < 1$, before the logarithmic function. (c) Post-habituating Model 2. The input signal is multiplied by a scalar, $\mu < 1$, after the logarithmic function. (d) Post-habituating Model 3. The two parameters of the logarithmic function are allowed to vary independently.

TABLE 1. Equations of the regression lines fit to difference-thresholds along the YV axis. The lines were fit separately to thresholds measured at judgment points on the positive side of white and to those on the negative side of white

Condition	$F \leq 0$	$F \geq 0$
+ ΔS probes, pre-habituation	$P = 0.002 - 0.159F$	$P = 0.001 + 0.791F$
+ ΔS probes, post-habituation	$P = 0.004 - 0.053F$	$P = 0.004 + 0.798F$
- ΔS probes, pre-habituation	$P = 0.002 - 0.117F$	$P = 0.002 + 0.446F$
- ΔS probes, post-habituation	$P = 0.003 - 0.001F$	$P = 0.004 + 0.515F$

The empirical values of the slope and the intercept were estimated from regression lines fit separately to pre-habituation threshold data on the two sides of W . The equations of these two lines are listed in Table 1. The intercept was estimated as the mean of the intercepts of the two regression lines. Since the data show a steeper slope on the positive side of W than on the negative side, β is greater on the positive side of W , giving a more compressed response function.

In Fig. 4 the solid lines indicate the fit of the pre-habituation model. The pre-habituation model predicts that the thresholds will increase in a straight line on either side of W . In this case, the model fits the data because the difference-thresholds are approximately a linear function of the flashed background. There are kinks in the predicted curves in the neighborhood of W that occur when the probe is of a different sign than the flash (e.g. a + ΔS probe from a judgment point on the negative side of W or a - ΔS probe from a judgment point on the positive side of W). Under these conditions, the threshold difference involves the two limbs of the response functions, simultaneously.

Three models for the effect of habituation

Model 1: multiplicative gain change before the logarithmic response function. In Model 1 [Fig. 5(b)] we assumed that the effect of habituation is to multiply the input to the logarithmic stage by a factor, $\nu < 1$. The response of the mechanism following habituation is R_ν , which can be written in terms of the pre-habituation response, R , as

$$R_\nu(C) = R(\nu C). \tag{11}$$

Assuming that threshold is based on a unit difference in the response, expressions can be derived for the predicted post-habituation thresholds, P_ν^* . For $F > 0$ and $P_\nu > 0$, this expression is

$$P_\nu^* = \frac{\hat{\alpha}}{\nu \hat{\beta}} (e^{\hat{\beta}} - 1) + (e^{\hat{\beta}} - 1)F, \tag{12}$$

where $\hat{\alpha}$ and $\hat{\beta}$ are the parameters for the pre-habituation response. The parameter ν can be evaluated from the data by comparing the expression for the intercept in equation (6) to the expression for the intercept in equation (12):

$$\hat{\nu} = \frac{\text{Intercept}_{\text{post}}}{\text{Intercept}_{\text{pre}}}. \tag{13}$$

Model 1 predicts that the post-habituation threshold curve will be shifted vertically from the pre-habituation curve by a value of $(1/\hat{\nu})$ while maintaining the same

slope. These predictions are shown in Fig. 4(a, b, c) as dotted lines. The prediction is acceptable for judgment points on the positive side of W , but not on the negative side of W .

Model 2: multiplicative gain change after the logarithmic response function. In Model 2 [Fig. 5(c)] we assumed that the effect of habituation is to multiply the input signal after the logarithmic stage by a factor, $\mu < 1$. The response of the mechanism following habituation is R_μ , which can be written in terms of the pre-habituation response, R , as

$$R_\mu(C) = \mu R(C). \tag{14}$$

Assuming that threshold is based on a unit difference in response, expressions can be derived for the predicted post-habituation thresholds, P_μ^* . For $F > 0$ and $P > 0$, this expression is

$$P_\mu^* = \frac{\hat{\alpha}}{\hat{\beta}} (e^{\hat{\beta}\mu} - 1) + (e^{\hat{\beta}\mu} - 1)F, \tag{15}$$

where $\hat{\alpha}$ and $\hat{\beta}$ are estimates for the pre-habituation response.

There are two ways that equation (15) could be used to estimate $\hat{\mu}$. One way is to equate $\text{Intercept}_{\text{post}}$ to

$$\frac{\hat{\alpha}}{\hat{\beta}} (e^{\hat{\beta}\mu} - 1)$$

and, from equation (10a), equate $\text{Intercept}_{\text{pre}}$ to

$$\frac{\hat{\alpha}}{\hat{\beta}} (e^{\hat{\beta}} - 1).$$

This gives

$$\hat{\mu} = \frac{\hat{\beta}}{\ln \left[\frac{\text{Intercept}_{\text{post}}}{\text{Intercept}_{\text{pre}}} (e^{\hat{\beta}} - 1) + 1 \right]}. \tag{16}$$

Another way of estimating μ is to equate $\text{Slope}_{\text{post}}$ to $(e^{\hat{\beta}\mu} - 1)$ and, from equation (10b), $\text{Slope}_{\text{pre}}$ to $(e^{\hat{\beta}} - 1)$. By this method,

$$\hat{\mu} = \frac{\hat{\beta}}{\ln \left[\frac{\text{Slope}_{\text{post}}}{\text{Slope}_{\text{pre}}} (e^{\hat{\beta}\mu} - 1) + 1 \right]}. \tag{17}$$

For Model 2 to be consistent with the data, equations (16) and (17) should give the same estimates for $\hat{\mu}$. For this to occur, the ratio of $\text{Intercept}_{\text{post}}$ over $\text{Intercept}_{\text{pre}}$ should equal the ratio of $\text{Slope}_{\text{post}}$ over $\text{Slope}_{\text{pre}}$; i.e. if the intercept increases, the slope of the threshold curve becomes proportionately steeper. On the YV axis, the intercept increases following habituation for both + ΔS and - ΔS probes, but the slope does not become steeper

relative to the pre-habituation curves. The predictions of Model 2 with $\hat{\mu}$ estimated from equation (16) are plotted in Fig. 4 (a, b, c) as dot-dashed lines. The predictions overestimate the slope of the data. If $\hat{\mu}$ had been estimated by the slope [i.e. from equation (17)], the predicted value of the post-habituation intercept would be too low. Hence, Model 2 can be rejected as an explanation of habituation effects along the *YV* axis.

Model 3: a change in the shape of the response function. Since neither Model 1 nor Model 2 is able to predict a shallower slope of the difference-threshold curve after habituation, we examined a third, more general model. In this model [Fig. 5(d)], exposure to a habituating light is allowed to change the two parameters of the logarithmic response function independently. The response of the mechanisms following temporal modulation is,

$$R_{\pi}(C) = \frac{1}{\beta_{\pi}} \ln(\alpha_{\pi} + \beta_{\pi}C) - \frac{1}{\beta_{\pi}} \ln(\alpha_{\pi}), \quad (18)$$

where α_{π} and β_{π} are the post-habituation parameters. Equation (18) has the same form as equation (3).

With the assumption that threshold is based on a unit response difference, expressions can be derived for the predicted post-habituation thresholds, P_{π}^* , similar to those from equations (6)–(9). For $F > 0$ and $P > 0$, this expression is

$$P_{\pi}^* = \frac{\alpha_{\pi}}{\beta_{\pi}} (e^{\beta_{\pi}} - 1) + (e^{\beta_{\pi}} - 1)F. \quad (19)$$

Empirical estimates for $\hat{\alpha}_{\pi}$, and $\hat{\beta}_{\pi}$ were obtained by equating the expressions for the slope and intercept to the equations from the regression lines that were fit to the post-habituation threshold curves.

The predictions of this model are shown in Fig. 4 (a, b, c) as dashed lines. It can be seen that for judgment points on the negative side of *W*, the fit is substantially better than that of either Model 1 or 2. However, the predicted curve on the positive side of *W* for $(-\Delta S)$ probes is not substantially different from that predicted by Model 1. Along the *YV* axis, then, the data can be described by a model in which the two parameters that control the shape of the non-linearity are affected independently by habituation.

EXPERIMENT 2: HABITUATION ALONG THE *RG* AXIS

In Exp. 2, thresholds were measured at judgment points spaced along the *RG* axis for probes that differed from the judgment point in the positive or negative direction along that axis. These thresholds were measured during adaptation to a white background, and following habituation to a light modulated along the length of the *RG* axis. A change from a light on the *RG* axis to any other light on the same axis causes equal and opposite changes in *L*- and *M*-cone excitation, but no change in *S*-cone excitation. In Fig. 6, therefore, the judgment points and difference-thresholds are represented in terms of a change in $(L - 1.94M)$ units,

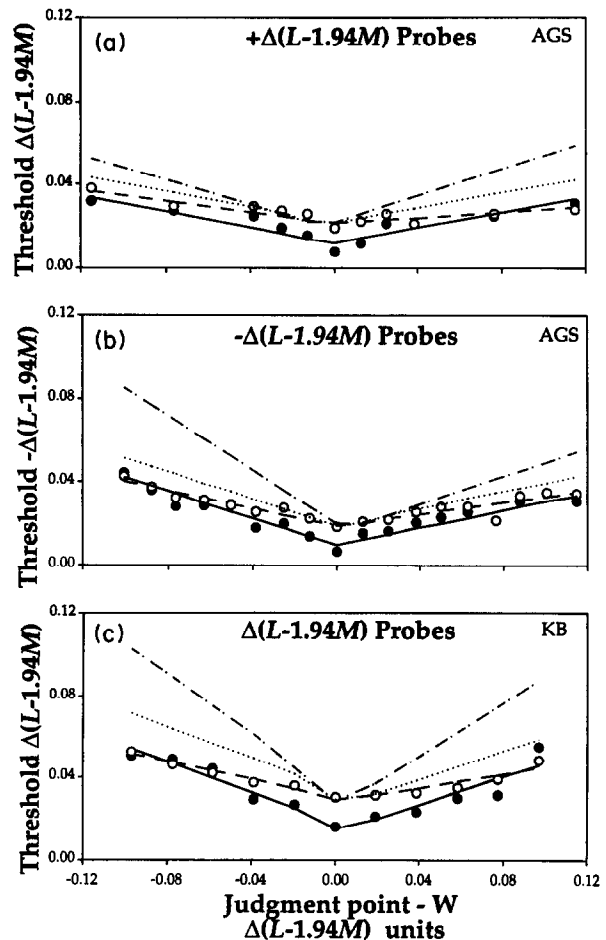


FIGURE 6. Difference-thresholds as a function of the judgment point's distance from *W* along the *RG* axis in $\Delta(L - 1.94M)$ units. (a) Difference-thresholds for probes differing from the judgment point in the positive direction of the *RG* axis. The solid circles indicate pre-habituation difference-thresholds; open circles indicate post-habituation difference-thresholds. The solid line represents the predictions of the pre-habituation model; the dotted line, of post-habituation Model 1; the dot-dashed line, of post-habituation Model 2; and the dashed line, of post-habituation Model 3. (b) The difference-thresholds that differ from the judgment point in the negative direction of the *RG* axis. The lines represent predictions from the same models re-evaluated for these probes. (c) A replication of the results on a second observer using bi-directional probes and a 2AFC task.

$\Delta(L - 1.94M)$. In Fig. 6(a) the thresholds are for probes that differ from the judgment point in the negative $\Delta(L - 1.94M)$ direction, and in Fig. 6(b), the positive $\Delta(L - 1.94M)$ direction. The solid circles are the pre-habituation thresholds, and the open circles are the post-habituation thresholds. The standard deviation of each point was between 10 and 20% of the threshold value.

The parameters of the models were estimated in the same manner as for the *YV* axis; i.e. the values of $\hat{\alpha}$ and $\hat{\beta}$ were estimated from the pre-habituation threshold curves, and the values of $\hat{\mu}$ and $\hat{\nu}$ from equations (13) and (16). The slope and intercept of the regression lines fit to the pre- and post-habituation thresholds used to generate these parameters are listed in Table 2.

The predictions of the pre-habituation model are shown as solid lines. For both $\Delta(L - 1.94M)$ and $-\Delta(L - 1.94M)$ probes, the fit of the model is tolerable.

TABLE 2. Equations of the regression lines fit to difference-thresholds along the *RG* axis. The lines were fit separately to thresholds measured at judgment points on the positive side of white and to those on the negative side of white

Condition	$F \leq 0$	$F \geq 0$
+ $\Delta(L - 1.94M)$ probes, pre-habituation	$P = 0.012 - 0.189F$	$P = 0.011 + 0.181F$
+ $\Delta(L - 1.94M)$ probes, post-habituation	$P = 0.022 - 0.131F$	$P = 0.021 + 0.063F$
- $\Delta(L - 1.94M)$ probes, pre-habituation	$P = 0.009 - 0.322F$	$P = 0.011 + 0.207F$
- $\Delta(L - 1.94M)$ probes, post-habituation	$P = 0.019 - 0.207F$	$P = 0.019 + 0.137F$

However, the difference-threshold curves bend downward at judgment points further away from *W*, creating small systematic deviations from the predicted straight line. It is probable that the probe interval is long enough for partial adaptation to increase sensitivity at the judgment point, and the effect is more noticeable when the flashed background is further from the adapting point.

The predictions of post-habituation Model 1 (scaling before the response function) are shown as dotted lines, and the predictions of post-habituation Model 2 (scaling after the response function) as dot-dashed lines. Model 1 predicts that the slopes of the post-habituation threshold curves should be the same as the slopes of the pre-habituation threshold curves. Model 2 predicts that the slopes of each branch of the curve should rise in proportion to the elevation of the threshold at white. Since the slopes of the post-habituation threshold curves are shallower than the slopes of the pre-habituation threshold curves, both of these models over-estimate the difference-thresholds. Even if one considers the slight bend in the curves, these models can not predict the habituation effects since the slopes of the post-habituation curves close to *W* are still flatter than those of the pre-habituation curves.

The predictions of post-habituation Model 3 (a change in shape of the response function) are shown as dashed lines. These predictions fit the post-habituation data because the difference-thresholds are approximately linear functions of the flash. The post-habituation response functions estimated for Model 3 are shallower and less compressive than those estimated from the pre-habituation data. Since the response functions are

shallower around the zero point, the post-habituation threshold at *W* is higher than the corresponding pre-habituation threshold, and since the response functions are less compressive, the post-habituation slopes are less steep. The data for the second observer [Fig. 6(c)] also rule out post-habituation Models 1 and 2.

EXPERIMENT 3: HABITUATION ALONG THE *LD* AXIS

In the third experiment, judgment points were spaced on the *LD* axis. During adaptation to a white background, and following habituation to a light modulated along the length of the *LD* axis, thresholds were measured for probes that differed from these points in the positive direction of the *LD* axis. Since there can be a substantial amount of brightness adaptation in 0.05 sec (Hayhoe, Benimoff & Hood, 1987), we used shorter durations for the flash and probes along the *LD* axis. The flashed field was presented for 0.025 sec, and the probe was presented simultaneously with the onset of the flash for 0.0083 sec (the shortest flash possible on our equipment). The durations of the adapting and habituating intervals were the same as in Fig. 2.

Figure 7 shows the difference-thresholds at each of the judgment points in terms of (*L* + *M* + *S*) units. The solid circles are the pre-habituation thresholds, and the open circles are the post-habituation thresholds. The pre-habituation threshold curve is minimum at *W* and then increases in proportion to the distance between the judgment point and *W*. On the positive side of *W* this increase is linear, but on the negative side of *W* there is a slight downward bend. The post-habituation threshold curve is higher than the pre-habituation threshold curve at *W*. The slopes of the threshold curve are flatter following habituation. At judgment points on the negative side of *W*, the post-habituation thresholds are lower than the pre-habituation thresholds. This branch of the post-habituation threshold curve is almost flat and does not show a downward bend.

The parameters of the models were estimated in the same manner as those of the *YV* and *RG* axes. The slopes and intercepts of the regression lines fit to the pre- and post-habituation threshold data are listed in Table 3. The predictions of the pre-habituation model are shown as a solid line. On the negative side of *W* this model can not account for the downward bend in the threshold curve at judgment points away from *W*, but it can predict the threshold curve on the positive side of *W*. The fit of post-habituation Model 1 (scaling before the response function) is shown as a dotted line and of

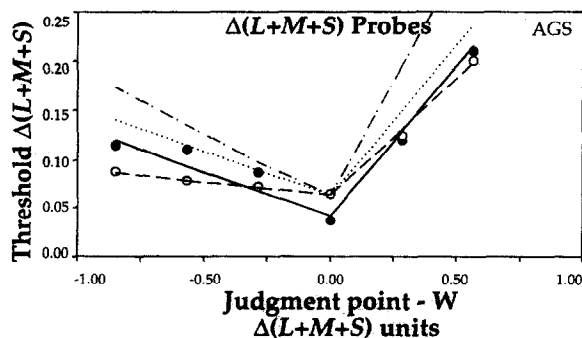


FIGURE 7. Difference-thresholds for (*L* + *M* + *S*) probes along the *LD* axis with shorter-duration flash and probe. The solid circles indicate pre-habituation difference-thresholds; open circles indicate post-habituation difference thresholds. The solid line represents the predictions of the pre-habituation model; the dotted line, of post-habituation model 1; the dot-dashed line, of post-habituation model 2; and the dashed line, of post-habituation Model 3.

TABLE 3. Equations of the regression lines fit to difference-thresholds along the LD axis. The lines were fit separately to thresholds measured at judgment points on the positive side of white and to those on the negative side of white

Condition	$F \leq 0$	$F \geq 0$
$\Delta(L + M + S)$ probes, pre-habituation	$P = 0.048 - 0.092F$	$P = 0.036 + 0.305F$
$\Delta(L + M + S)$ probes, post-habituation	$P = 0.064 - 0.028F$	$P = 0.062 + 0.238F$

post-habituation Model 2 (scaling after the response function), as a dot-dashed line. Since the slopes of the post-habituation threshold curves are shallower than the pre-habituation curves, neither Model 1 nor Model 2 can describe the habituation effects. The fit of post-habituation Model 3 (a change in shape of the response function) is shown as a dashed line. The post-habituation response functions estimated for Model 3 are shallower and less compressive than those estimated from the pre-habituation data. This leads to a threshold curve that is elevated at W and has a flatter slope than the pre-habituation curve. The predictions from Model 3 provide a good fit to the data.

HABITUATION VERSUS ADAPTATION TO STEADY LIGHTS

Habituation to a light modulated along a cardinal axis elevates thresholds for probes that differ from W along the same cardinal axis. Thresholds for the same probes are also elevated if the steady adapting light is shifted from W to another light on the same cardinal axis (Krauskopf, Williams, Mandler & Brown, 1986; Shapiro *et al.*, 1990; Zaidi *et al.*, 1992). However, just because these two conditions elevate thresholds at W , it is not sufficient to conclude that habituation and adaptation change sensitivity by affecting the same underlying processes. In this part of the study, we compared the change in difference-threshold curves due to habituation, to those due to a shift in the color of a steady adaptation light. The additional information provided by the thresholds on flashed backgrounds enabled us to show that the effects of habituation are different from the effects of a change in steady adaptation.

Procedure for adaptation experiments

The difference-threshold curves measured under different states of adaptation discussed in this section are taken from Shapiro *et al.* (1990) and Zaidi *et al.* (1992). In these studies difference-threshold curves were measured using the same spatial configuration and temporal sequence as the pre-habituation condition shown in Fig. 3(a). The only difference was that threshold curves were measured not only during adaptation to W , but also during adaptation to colors represented by other points on the YV and RG axes. The data shown are for one of the authors (AGS). Results on each of the axes have been replicated on one other color-normal observer.

Figure 8(a) shows three difference-threshold curves, each measured during steady adaptation to different steady backgrounds along the YV axis. The thresholds

are for $-\Delta S$ probes measured at judgment points along the YV axis. For all three curves, the judgment points are expressed in ΔS units from W , and the thresholds in $-\Delta S$ units from the judgment point. The adaptation points are indicated by the arrows at the bottom of the horizontal axis. The solid circles show difference-thresholds measured during adaptation to a steady white field; the open squares, difference-thresholds measured during adaptation to a steady yellow light (arrow at -0.009); and the open triangles, difference-thresholds measured during adaptation to a steady violet light (arrow at 0.009). Straight lines have been used to connect the points for each condition for visual convenience. These curves should be compared to the pre- and post-habituation curves in Fig. 4(b).

Figure 8(b) shows three difference-threshold curves for $-\Delta(L - 1.94M)$ probes measured at judgment

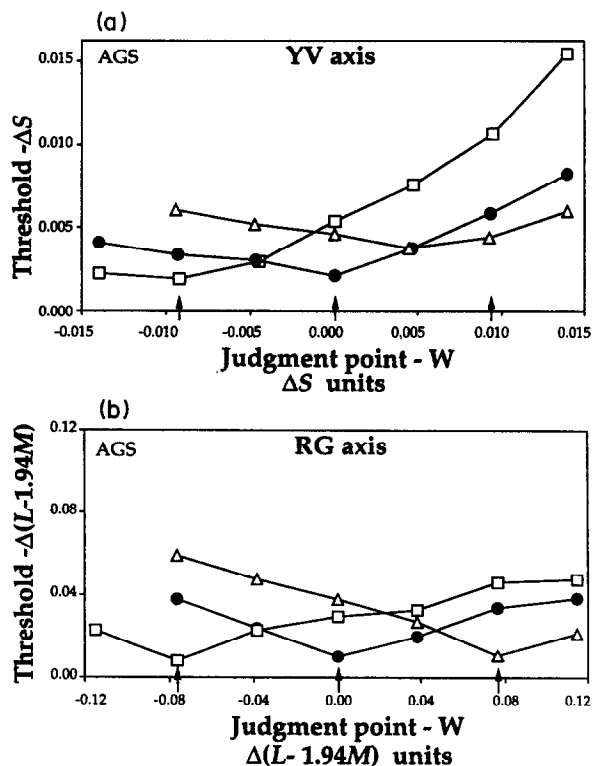


FIGURE 8. The effects of steady adaptation level on difference thresholds along the YV and RG axes. (a) The threshold curves measured along the YV axis during adaptation to the backgrounds indicated by the arrows on the x-axis: the open squares, arrow at -0.009 ; the solid circles, arrow at W ; the open triangles, arrow at 0.009 . These curves can be compared to the effects of habituation in Fig. 4(b). (b) Threshold curves measured along the RG axis during adaptation to the backgrounds indicated by the arrows: the open squares, arrow at -0.076 ; the solid circles, arrow at W ; the open triangles, arrow at 0.076 . These curves can be compared to the effects of habituation in Fig. 6(b). The points are connected by straight lines for visual convenience.

points on the RG axis. Each curve was measured during adaptation to a different steady background on the RG axis. For all three curves, the judgment points are expressed in $\Delta(L - 1.94M)$ units from W , and the thresholds in $-\Delta(L - 1.94M)$ units from the judgment point. The solid circles indicate difference-thresholds measured during adaptation to a steady white field; the open squares, difference-thresholds measured during adaptation to a steady green light (arrow at -0.076); and the open triangles, difference-thresholds measured during adaptation to a steady red light (arrow at 0.076). Straight lines have been used to connect the points for each condition for visual convenience. These curves should be compared to the pre- and post-habituation curves in Fig. 6(b).

Thresholds are elevated at W both during adaptation to the non-white backgrounds and after habituation to temporal modulation. These elevations, however, are due to different patterns of change in the difference-threshold curves. Following steady adaptation, there is a lateral shift in the threshold curve so that the minimum is at, or near, the point of steady adaptation. A consequence of this shift is that difference-thresholds measured at points away from the adapting light will be elevated. Following habituation, however, the minimum of the threshold curve is not shifted significantly from W ; instead, the whole curve is raised and the slope flattened. This makes the threshold elevation greatest at W .

The shift in sensitivity following exposure to different steady adaptation backgrounds requires a different explanation than do the changes observed following habituation. The lateral shift in the chromatic threshold curves can be explained by an imbalance due to independent adaptive processes in the pre-opponent paths (Zaidi *et al.*, 1992). An explanation of adaptation along the RG line may also require an additional post-opponent adaptive process (Shapiro *et al.*, 1990; Krauskopf & Gegenfurtner, 1991). Because habituation along the LD axis has no effect on the thresholds along the RG axis, pre-opponent response changes do not play a role in habituation (Krauskopf *et al.*, 1982). The types of processes affected by changes in steady adaptation, then, differ from those affected by habituation.

SUMMARY AND DISCUSSION

In order to assess the effects of habituation on the cardinal mechanisms, we measured difference-thresholds at judgment points along the cardinal axes before and after habituation. The threshold curves measured before habituation were described by a model based on a logarithmic input-response relationship. The parameters controlling the shape of this logarithmic response function were estimated from regression lines fit to pre-habituation curves on both sides of W . We then examined the predictions of three simple models that could describe the effects of habituation. The first two models multiplied the signal at different stages while

maintaining the parameters of the logarithmic response function estimated from the pre-habituation data. In post-habituation Model 1 a multiplicative gain control was placed before the logarithmic response function. This model predicted that the threshold at W would be elevated, while the slopes of the post-habituation threshold curves would be parallel to the slopes pre-habituation threshold curves. With the exception of positive branches along the YV axis, this model could not describe the data. In post-habituation Model 2 a multiplicative gain control was placed after the logarithmic response function. This model predicted that the slopes of the post-habituation threshold curves would be steeper in proportion to the increase in threshold at W . Since the slopes of the post-habituation threshold curves are shallower than the pre-habituation curves, this model was also shown to be inadequate.

While these two multiplicative models could not describe the threshold data, a more general model (Model 3) predicted the effects of habituation by re-estimating the two parameters of the logarithmic response function. Model 3 was capable of describing post-habituation thresholds along all three of the cardinal axes. However, since the parameters were re-estimated independently of the pre-habituation threshold curves, this model could predict any curve in which the thresholds increased proportionately to the judgment point's distance from W . This model is just a description of the change in thresholds. At present we do not have a theory about this change. Habituation leads to a flatter response function, thus elevating the threshold at W , while increasing the approximately linear range of the mechanism.

The psychophysical results of this study can stand on their own. However, it is interesting that electrophysiological measurements also indicate that the effects of habituation on the response of cortical neurons can not be explained by a multiplicative change in the signal. Movshon and Lennie (1979) measured the contrast-response function of single cells in the cat central visual cortex before, during, and after prolonged exposure to drifting sinusoidal gratings. Exposure to drifting gratings leads to a modulation of the response of simple cells, and thus is analogous to our habituation procedure. They found that a decrease in sensitivity can be specific to the spatial frequency of the adapting stimulus, implying that the effects of habituation for individual cells should not be thought of as a multiplicative scaling of an invariant spatial frequency-response function, but rather a process which changes the shape of the function. In general the effect of habituation was to flatten the contrast-response function. Sclar, Lennie and DePriest (1989) compared the contrast-response function of cortical cells in macaques before and during habituation by fitting each curve with a Naka-Rushton function. Their results were complicated, but in general they found that changes in the contrast-response function following habituation for most cells could be accounted for only by changing both the semi-saturation constant and the exponential parameter.

We also compared the effects of habituation to those measured following a shift in steady adaptation (Fig. 8). Following habituation, the difference-threshold curves were elevated at W and flatter than before habituation, whereas after adaptation to a steady non-white field, the difference-threshold curves were translated laterally so that the location of the minimum threshold was at, or near, the adapting light [see Craik (1938) for similar shifts in brightness-threshold curves]. Since thresholds at W were elevated following both habituation and steady adaptation, the major differences in the two effects are seen at judgment points away from W . Thus, by measuring a larger range of difference-thresholds, we were able to differentiate processes that appear similar when only thresholds at W are considered. From this comparison it seems likely that these two types of conditioning stimuli affect two different types of underlying processes.

It is easy to see the utility of processes that adapt an observer's visual system to the mean level of light incident from an image. The observer becomes maximally sensitive to changes around the mean level, thus matching sensitivity to the range of lights that are actually present in the image. This shift in sensitivity is also useful because the range of possible lights that can be encountered in different situations is much larger than the range of sensitivity in any particular state of adaptation (Craik, 1938).

It is more difficult to speculate on the functional advantage of habituating to prolonged temporal modulation. Habituation experiments, however, have demonstrated the existence of color mechanisms that change their sensitivity in response to repeated temporal transitions of the input. A modification of the sinusoidal habituation experiment was used by Krauskopf *et al.* (1982) and Krauskopf and Zaidi (1986) to show that habituation reduces sensitivity to color transitions *per se* rather than to color differences. The habituating stimulus in these experiments was a uniform disk whose color was modulated around mid-white as a temporal sawtooth along a cardinal axis, and the tests were step changes in the color of the disk from mid-white towards the two ends of the habituating color line. The results showed that thresholds for detecting step changes in opposite directions along a color line could be selectively elevated. For example, after habituating to a light modulated along the RG line, when the ramp phase of the sawtooth went from "red" to "green," thresholds for "green" steps were elevated more than thresholds for "red" steps. Likewise, when the sign of the sawtooth was reversed, thresholds for "red" steps were elevated more than thresholds towards "green." The selective elevation of thresholds in complementary directions cannot be explained within the framework of traditional first- and second-stage color mechanisms. It can be explained, however, by postulating mechanisms that respond to change in one color direction but not to change in its complementary direction. The functional nature of these mechanisms has been explored by Zaidi and Halevy (1991, 1992). The results of the present study show that

the effect of prolonged temporal modulation on the differential response of these mechanisms is complex and cannot be encapsulated in a notion of "fatigue" or by a simple multiplicative gain change.

REFERENCES

- Adelson, E. H. (1982). Saturation and adaptation of the rod system. *Vision Research*, 22, 1299–1312.
- Craik, K. J. W. (1938). The effect of adaptation on differential brightness discrimination. *Journal of Physiology*, 92, 406–421.
- Geisler, W. S. (1979). Initial image and after-image discrimination in the human rod and cone system. *Journal of Physiology*, 294, 165–179.
- Hayhoe, M. M., Benimoff, N. I. & Hood, D. C. (1987). The time course of multiplicative and subtractive adaptation processes. *Vision Research*, 27, 1981–1996.
- Hood, D. C., Finkelstein, M. A. & Buckingham, E. (1979). Psychophysical tests of models of the response function. *Vision Research*, 19, 401–406.
- Krauskopf, J. & Gegenfurtner, K. (1991). Adaptation and color discrimination. In Valberg, A. & Lee, B. B. (Eds), *Pigments to perception* (pp. 379–390). New York: Plenum Press.
- Krauskopf, J. & Zaidi, Q. (1986). Induced desensitization. *Vision Research*, 26, 1752–1757.
- Krauskopf, J., Williams, D. & Heeley, D. (1982). Cardinal directions of color space. *Vision Research*, 22, 1123–1131.
- Krauskopf, J., Williams, D. R., Mandler, M. B. & Brown, A. M. (1986). Higher order color mechanisms. *Vision Research*, 26, 23–32.
- Loomis, J. M. & Berger, T. (1979). Effects of chromatic adaptation on color discrimination and color appearance. *Vision Research*, 19, 891–901.
- MacLeod, D. I. A. & Boynton, R. M. (1979). Chromaticity diagram showing cone excitation by stimuli of equal luminance. *Journal of the Optical Society of America A*, 69, 1183–1186.
- Movshon, J. A. & Lennie, P. (1979). Pattern-selective adaptation in visual cortical neurones. *Nature*, 278, 850–852.
- Sachtler, W. & Zaidi, Q. (1992). Chromatic and luminance signals in visual memory. *Journal of the Optical Society of America A*, 9, 877–894.
- Scialo, G., Lennie, P. & DePriest, D. D. (1989). Contrast adaptation in striate cortex of Macaque. *Vision Research*, 29, 747–755.
- Shapiro, W., Zaidi, Q. & Hood, D. C. (1990). Adaptation in the red-green (L-M) color system. *Investigative Ophthalmology and Visual Science (Suppl.)*, 31, 262.
- Smith, V. C. & Pokorny, J. (1975). Spectral sensitivity of the foveal cone photopigments between 400 and 500 nm. *Vision Research*, 15, 161–171.
- Wetherill, G. B. & Levitt, H. (1965). Sequential estimation of points on a psychometric function. *British Journal of Mathematical and Statistical Psychology*, 18, 1–10.
- Wright, W. D. (1935). Intensity discrimination and its relation to the adaptation of the eye. *Journal of Physiology*, 83, 466–477.
- Zaidi, Q. & Halevy, D. (1991). Chromatic mechanisms beyond linear opponency. In Valberg, A. & Lee, B. B. (Eds), *Pigments to perception* (pp. 337–348). New York: Plenum Press.
- Zaidi, Q. & Halevy, D. (1992). Visual mechanisms that signal the direction of color changes. *Vision Research* Submitted.
- Zaidi, Q. & Hood, D. (1988). Sites of instantaneous non-linearities in the visual system. *Investigative Ophthalmology and Visual Science (Suppl.)*, 29, 163.
- Zaidi, Q., Shapiro, A. G. & Hood, D. C. (1992). The effect of adaptation on the differential sensitivity of the S-cone color system. *Vision Research*, 32, 1297–1318.

Acknowledgements—We would like to thank Sherri Geller for help in editing the text and Karen Burhans for patient observation. This research was partially supported by the National Eye Institute through grant EY07556 to Q. Zaidi.